

Orbital Isotropy of Magnetic Fluctuations in Correlated Electron Materials Induced by Hund's Exchange Coupling

Evgeny A. Stepanov,^{1,2} Yusuke Nomura,³ Alexander I. Lichtenstein,^{1,2} and Silke Biermann^{4,5}

¹*Institute of Theoretical Physics, University of Hamburg, Jungiusstrasse 9, 20355 Hamburg, Germany*

²*Theoretical Physics and Applied Mathematics Department,*

Ural Federal University, Mira Str. 19, 620002 Ekaterinburg, Russia

³*RIKEN Center for Emergent Matter Science, 2-1 Hirosawa, Wako, Saitama 351-0198, Japan*

⁴*CPHT, CNRS, Ecole Polytechnique, Institut Polytechnique de Paris, F-91128 Palaiseau, France*

⁵*Collège de France, 11 place Marcelin Berthelot, 75005 Paris, France*

Characterizing non-local magnetic fluctuations in materials with strong electronic Coulomb interactions remains one of the major outstanding challenges of modern condensed matter theory. In this work we address the spatial symmetry and orbital structure of magnetic fluctuations in perovskite materials. To this aim, we develop a consistent multi-orbital diagrammatic extension of dynamical mean field theory, which we apply to an anisotropic three-orbital model of cubic t_{2g} symmetry. We find that the form of spatial spin fluctuations is governed by the local Hund's coupling. For small values of the coupling, magnetic fluctuations are anisotropic in orbital space, which reflects the symmetry of the considered t_{2g} model. Large Hund's coupling enhances collective spin excitations, which mixes orbital and spatial degrees of freedom, and magnetic fluctuations become orbitally isotropic. Remarkably, this effect can be seen only in two-particle quantities; single-particle observables remain anisotropic for any value of the Hund's coupling. Importantly, we find that the orbital isotropy can be induced both, at half-filling and for the case of 4 electrons per lattice site, where the magnetic instability is associated with different, antiferromagnetic and ferromagnetic modes, respectively.

An accurate description of many-body effects in multi-orbital systems represents a challenging task for theoretical condensed matter physics. In addition to collective charge, spin and superconducting fluctuations that are present already in effective single-orbital systems, realistic materials possess orbital degrees of freedom, which greatly enhances the wealth of the physical phenomena displayed by such materials. In strongly interacting electronic systems these fluctuating degrees of freedom become entangled, and it is difficult to foresee which collective effects govern the physics of the system.

Perovskite materials with partially filled t_{2g} orbitals reveal a high degree of anisotropy and may serve as an attractive playground for studying the interplay between orbital and spin degrees of freedom [1]. Prominent examples are LaTiO_3 , SrRuO_3 and, to a lesser degree, Sr_2RuO_4 . In these materials, strong magnetic fluctuations have been revealed by inelastic neutron scattering experiments [2–7]. For LaTiO_3 , it has been argued that the joint effect of the superexchange interaction and the Hund's exchange coupling leads to a disordered orbital ground state [8]. Despite antiferromagnetic superexchange interactions, SrRuO_3 is an itinerant ferromagnet. It undergoes a Curie transition at $T_c = 160$ K [9], which is accompanied by a distortion of the ideal cubic perovskite structure (see e.g. Ref. 10). While the formation of the ferromagnetic state in this material can be well captured within *ab initio* density functional calculations [11–13], description of itinerant ferromagnetism above T_c is challenging and requires consideration of long-range collective electronic fluctuations. In Sr_2RuO_4 , coupling of Hund's exchange to orbital degrees of freedom was found to be responsible for the magnetic fluctuations [14–19]. Quite generally, anisotropies in correlated systems may favor instabilities of various nature, such as orbital ordering [20], Peierls instabilities [21], strong crystal-

field splitting [22], and Fermi-surface instabilities related to the Pomeranchuk effect [23]. The theoretical description of this phenomenology is hindered by the fact that local approximations to electronic Coulomb correlations tend to overestimate anisotropies of a system. Indeed, taking into account long-range fluctuations may drastically change the physical picture [24]. Nevertheless, even most recent works on correlated multi-orbital systems are based on dynamical mean-field (DMFT) calculations [25–27], illustrating the lack of computationally tractable approaches beyond the local picture.

In this work we address the problem of spin fluctuations in perovskite materials close to a magnetic instability, using a realistic three-orbital t_{2g} model. We find that non-local spin fluctuations enhanced by large Hund's exchange coupling strongly reduce the orbital anisotropy of the perovskite structure. As a consequence, magnetic fluctuations become isotropic in orbital space, as we show both at half-filling, as well as for the case of 4 electrons per lattice site. These results illustrate the important role that the local Hund's coupling plays not only for the local spin physics, but also for the symmetry and orbital structure of spatial magnetic excitations. A second important result of our work is the design of a minimal consistent multi-orbital extension of the recently introduced dual triply irreducible local expansion (D-TRILEX) approach [28, 29]. The D-TRILEX has a diagrammatic structure similar to *GW* [30–32], which allows for a self-consistent consideration of the feedback of collective electronic fluctuations onto the single-particle quantities and *vice versa*. However, in contrast to *GW*, our method allows for a simultaneous and unambiguous accounting for leading collective electronic effects including magnetic fluctuations in a simple partially bosonized way [28, 33, 34]. Moreover, these many-body effects can be considered as true long-range fluctuations with-

out any spatial restrictions, which is a decisive advantage over cluster extensions of DMFT [35–40]. Finally, the D-TRILEX approach accounts for the exact local three-point vertex corrections at both sides of the GW -like diagrams for the self-energy and polarization operator, which preserves correct orbital structure of spatial fluctuations. These vertices are crucial for describing the isotropic nature of the spin fluctuations described above: in their absence, this physics is not even qualitatively captured.

Model — We start with a realistic t_{2g} tight-binding model for the perovskite materials described by the three-orbital Hamiltonian

$$\mathcal{H} = - \sum_{ij,l,\sigma} t_{ij}^l c_{i\sigma}^\dagger c_{j\sigma} + \frac{1}{2} \sum_{i,l'} \left(U_{l'}^{\text{ch}} n_{i\uparrow} n_{i\downarrow} + U_{l'}^{\text{sp}} m_{i\uparrow} m_{i\downarrow} \right), \quad (1)$$

where operator $c_{i\sigma}^{(\dagger)}$ annihilates (creates) an electron with spin projection $\sigma = \{\uparrow, \downarrow\}$ on site i and orbital $l = \{1, 2, 3\}$. The anisotropy of this model originates from hopping parameters t_{ij}^l that are diagonal in the orbital space and have the following structure in momentum (\mathbf{k}) space [41]

$$t_{il}(\mathbf{k}) = \epsilon + 2t_\pi(C_\alpha + C_\beta) + 2t_\delta C_\gamma + 4t_\sigma C_\alpha C_\beta, \quad (2)$$

where ϵ is the center of bands and $C_\alpha = \cos k_\alpha$. For simplicity, we introduce three non-equivalent α, β, γ indices, where the first two are defined by the orbital label $l = \{\alpha\beta\}$ with $1 = yz$, $2 = zx$, and $3 = xy$. The last index γ takes the remaining value among $\{x, y, z\}$. In this model, orbital degrees of freedom are tied to a spatial motion of the electrons, because the latter can hop only within the same orbital in a strictly defined direction, which is different for every considered orbital. The $t_{\pi,\delta,\sigma}$ matrix elements describe the main hopping processes that provide the t_{2g} symmetry. We choose $t_\pi = 1$, which defines the energy scale of the system, and a realistic value for $t_\delta = 0.12$ for the SrVO₃ perovskite [41]. We note that t_σ plays the role of t' in a two-dimensional model for cuprates and shifts the van-Hove singularity (vHS) away from the Fermi level. The presence of the vHS at the Fermi energy results in a peak in the density of states, which enhances correlation effects in the system. Thus, for the half-filled case ($\langle N_i \rangle = 3$ electrons per site) we preserve the particle-hole symmetry for t_{2g} bands and set $t_\sigma = 0$. For the case of $\langle N_i \rangle = 4$ we choose the positive value for $t_\sigma = 0.35$ [41], which ensures that the vHS again appears at the Fermi level [42].

The on-site charge and spin density operators are defined as $n_{il} = n_{i\uparrow} + n_{i\downarrow}$ and $m_{il} = n_{i\uparrow} - n_{i\downarrow}$, where $n_{i\sigma} = c_{i\sigma}^\dagger c_{i\sigma}$. The interaction is parametrized in the Kanamori form [43] with intraorbital U and interorbital U' Coulomb interactions, and the Hund's coupling J . This parametrization is rotationally invariant provided $U' = U - 2J$. Given that the matrix of hopping amplitudes is diagonal in orbital space, we consider only the density-density part of the Kanamori interaction

$$2U^{\text{ch}} = \begin{pmatrix} U & U^* & U^* \\ U^* & U & U^* \\ U^* & U^* & U \end{pmatrix}, \quad 2U^{\text{sp}} = \begin{pmatrix} -U & -J & -J \\ -J & -U & -J \\ -J & -J & -U \end{pmatrix}, \quad (3)$$

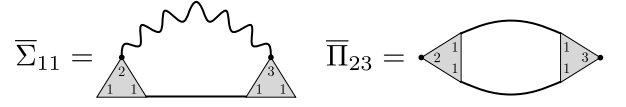


FIG. 1. Diagrams for the non-local self-energy $\bar{\Sigma}_{ll}$ and polarization operator $\bar{\Pi}_{ll'}$. Grey triangles correspond to full local vertex functions $\Lambda_{ll'}$ of DMFT impurity problem. Wiggly line depicts the renormalized interaction $W_{ll'}$. Other bold lines are dressed non-local Green's functions \bar{G}_{ll} . Labels $l = \{1, 2, 3\}$ are orbital indices. Summation over internal orbital indices is implied.

where $U^* = 2U' - J$. This expression for the interaction between charge and spin densities can be obtained rewriting the intraorbital Coulomb potential in the Ising-like form

$$U n_{i\uparrow} n_{i\downarrow} = \frac{U}{4} (n_{i\uparrow} n_{i\downarrow} - m_{i\uparrow} m_{i\downarrow}). \quad (4)$$

As has been shown recently, this decoupling provides a relatively good result for the self-energy [28, 44].

Many-body effects — The non-interacting part of the problem (1) is highly anisotropic. We find, however, that many-body interactions can drastically change this property of the system. In this work collective electronic fluctuations are taken into account via the simplest consistent diagrammatic extension of DMFT [45], which yet allows to consider desirable lowest-order vertex corrections without heavy numerical efforts. This theory is formulated as a multi-orbital extension of the D-TRILEX approach [28, 29] that has been introduced recently as a simplified version of the dual boson (DB) theory [46–51]. Both methods use DMFT as a starting point for diagrammatic expansion. Thus, the local self-energy $\Sigma_{ll}^{\text{imp}}(\nu)$ and polarization operator $\Pi_{ll'}^{\text{imp}}(\omega)$ are given by an effective impurity problem of DMFT-type. To avoid double-counting issues, the diagrammatic part of the theory that accounts for spatial correlation effects is formulated in a dual space. To this aim, we perform a transformation of initial fermionic variables and exactly integrate out the local impurity problem [28]. This allows to construct an analog of the Almladh functional [52] in the dual space $\Psi[\bar{G}, W^\zeta, \Lambda^\zeta] = \frac{1}{2} \bar{G}_{ll} \Lambda_{ll'}^\zeta W_{ll'}^\zeta \Lambda_{ll'}^{*\zeta} \bar{G}_{ll}$, which guarantees consistency between single- and two-particle quantities by means of the non-local self-energy and polarization operator

$$\bar{\Sigma}_{ll}(k) = - \sum_{q, l', \zeta} \bar{G}_{ll}(k+q) \Lambda_{ll'}^\zeta(\nu, \omega) W_{ll'}^\zeta(q) \Lambda_{ll'}^{*\zeta}(\nu, \omega) \quad (5)$$

$$\bar{\Pi}_{ll'}^\zeta(q) = 2 \sum_{k, l} \Lambda_{ll'}^{*\zeta}(\nu, \omega) \bar{G}_{ll}(k+q) \bar{G}_{ll}(k) \Lambda_{ll'}^\zeta(\nu, \omega) \quad (6)$$

Labels $k = \{\mathbf{k}, \nu\}$ and $q = \{\mathbf{q}, \omega\}$ describe momentum \mathbf{k} (\mathbf{q}) and Matsubara fermion ν (boson ω) frequency dependence. $\bar{G}_{ll}(k) = G_{ll}(k) - g_{ll}(\nu)$, where $g_{ll}(\nu)$ is the local part of the lattice Green's function $G_{ll}(k)$. $W_{ll'}^\zeta(q)$ is the renormalized interaction in the charge ($\zeta = \text{ch}$) and spin ($\zeta = \text{sp}$) channel. These quantities can be obtained self-consistently via standard Dyson equations $G_{ll}^{-1}(k) = i\nu + \mu - t_{ll}(\mathbf{k}) - \Sigma_{ll}(k)$ and $W_{ll'}^{\zeta-1}(q) = U_{ll'}^{\zeta-1} - \Pi_{ll'}^\zeta(q)$, where μ is the chemical potential,

and $\Sigma_{ll}(k) = \Sigma_{ll}^{\text{imp}}(\nu) + \bar{\Sigma}_{ll}(k)$ and $\Pi_{l'l''}(q) = \Pi_{l'l''}^{\text{imp}}(\omega) + \bar{\Pi}_{l'l''}(q)$ are the total self-energy and polarization operator, respectively [53]. In this way, the D-TRILEX theory provides an equal footing description of collective charge and spin fluctuations. The susceptibility $X_{ll}^S(q)$ in the corresponding channel, which is an experimentally observable quantity, can also be obtained via Dyson's equation $X_{ll}^{S-1}(q) = \Pi_{ll}^{S-1}(q) - U_{ll}^S$.

Finally, it is worth noting that the introduced improved GW-like form for the non-local self-energy (5) and polarization operator (6) additionally accounts for vertex corrections at both sides of the corresponding diagrams [54]. $\Lambda_{ll}^S(\nu, \omega)$ is the full local three-point vertex given by the DMFT impurity problem, and the quantity $\Lambda_{ll}^{*S}(\nu, \omega) = \Lambda_{ll}^S(\nu + \omega, -\omega)$ is introduced to simplify notations. As Fig. 1 demonstrates, this form of the diagrams allows to preserve correct orbital symmetry of electronic fluctuations. Indeed, the orbital structure of both lattice sites that are connected by the non-local Green's function \bar{G} is considered in a symmetric way, which is missing in the original TRILEX approach [55, 56]. It should be noted that the full local vertex function Λ_{ll} serves as the bare interaction vertex in the renormalized perturbation D-TRILEX theory [28, 29]. Therefore, the introduced diagrammatic structures (5) and (6) do not contradict the exact Hedin form for the self-energy and polarization operator [30]. As has been clarified in Ref. 49, both of these expressions can be identically rewritten in the conventional Hedin form that contains a non-local vertex function at one side of the diagram.

A particular symmetry of the considered model (1) allows us to use a simplified version of the multi-orbital D-TRILEX approach [57], where the vertex function Λ_{ll} and renormalized interaction $W_{l'l''}$ are taken in the density-density form and depend on two orbital indices instead of four. This makes the dressed Green's function G_{ll} diagonal in the orbital space and thus anisotropic. However, as we shall see later, the initial single-particle anisotropy of the model (2) does not necessarily extend to two-particle quantities. Indeed, although the Green's function is diagonal, the presence of vertex corrections Λ_{ll} leads to non-diagonal contributions to the non-local polarization function (6). Further, a matrix structure of the Dyson equation for the renormalized interaction W_{ll} and the susceptibility X_{ll} even more entangles orbital and spatial degrees of freedom. In this way, strong non-local collective fluctuations, which are magnetic in our particular case, can destroy the spatial anisotropy in the orbital space. This observation suggests to reconsider the commonly believed mean-field-based statement that correlations usually tend to increase the anisotropy of a system.

Orbital isotropy of magnetic fluctuations — Remarkably, we find that the strength and orbital structure of spatial magnetic fluctuations are controlled by the value of the local Hund's coupling J . To illustrate this point, let us first consider the interacting three-orbital model (1) at half-filling with $U = 4$ and temperature $T = 1/2$. For the specified parameters, the leading eigenvalue (i.e.) λ of the Dyson equation for the susceptibility X_{ll} indicates that strongest collective excitations in the system correspond to a magnetic instability chan-

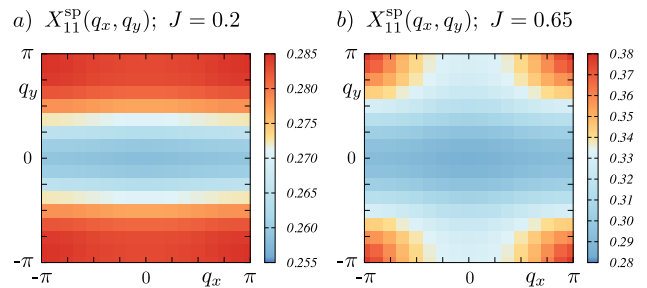


FIG. 2. The absolute value of the diagonal yz orbital component of the spin susceptibility $X_{11}^{\text{sp}}(q_x, q_y; q_z = 0, \omega = 0)$ obtained for the half-filled t_{2g} model for $U = 4$. Color bars show the strength of X^{sp} . (a) In the case of small Hund's coupling $J = 0.2$, the diagonal component of the susceptibility is highly anisotropic and is almost dispersionless along q_x direction. (b) Increasing the Hund's coupling to $J = 0.65$, intraorbital spin fluctuations become isotropic with a pronounced antiferromagnetic behavior depicted by the largest value of X_{11}^{sp} at corners of the Brillouin zone.

nel. We observe that for a relatively small $J = 0.2$, the i.e. of magnetic fluctuations is not very large ($\lambda = 0.78$). In this case, the diagonal (intraorbital) part of the spin susceptibility X_{ll}^{sp} presented in Fig. 7a for the yz orbital is much larger than the non-diagonal (interorbital) one shown in the Supplemental Material (SM) [58]. Moreover, the $X_{11}^{\text{sp}}(q_x, q_y; q_z = 0, \omega = 0)$ component of the susceptibility is highly anisotropic in momentum space and is almost dispersionless along q_x direction. This spatial structure of the spin susceptibility originates from the orbital symmetry of t_{2g} hopping processes (2). The same symmetry also leads to the identical q_y and q_z momentum dependence of $X_{11}^{\text{sp}}(\mathbf{q})$. Importantly, all three diagonal components X_{11}^{sp} , X_{22}^{sp} , and X_{33}^{sp} of the susceptibility show a similar behavior in momentum space with a pronounced dispersionless structure along q_x , q_y and q_z directions, respectively. This result indicates that for small Hund's coupling, orbital degrees of freedom are anisotropic.

Increasing the value of the Hund's coupling to $J = 0.65$, the magnetic i.e. approaches unity ($\lambda = 0.99$), which indicates that spin fluctuations are strongly enhanced [59]. This can also be concluded from Fig. 7 comparing the amplitude of the susceptibility for two considered cases of J . Moreover, at this large value of the Hund's coupling interorbital components of X^{sp} (see SM [58]) become comparable to intraorbital ones (Fig. 7b). This is the first signature of the isotropic orbital behavior of magnetic fluctuations. A proximity of the i.e. to unity indicates that all orders of an effective perturbation expansion given by the Dyson equation contribute almost equally to the total X^{sp} . This leads to a more thorough mixing of orbital and spatial degrees of freedom in the susceptibility. As shows Fig. 7b, this results in a highly isotropic form of spin fluctuations with a clearly distinguishable antiferromagnetic (AFM) behavior. Interorbital components of the susceptibility remain isotropic in momentum space [58]. This means, that orbital degrees of freedom are no more tied to a specific spatial direction defined by hopping parameters (2) of

the considered model. As a consequence, collective fluctuations in the magnetic channel become orbitally isotropic.

Remarkably, the non-local part of the dressed Green's function shown in the SM [58] remains spatially anisotropic for both considered cases of the Hund's coupling. This can be explained by the fact that the bare Green's function is highly anisotropic and isolates only the anisotropic contribution from the non-local self-energy (5), despite that the renormalized interaction $W_{\nu\nu'}^{\text{sp}}$ can be isotropic. Therefore, the orbital isotropy induced by strong magnetic fluctuation can be revealed only in two-particle quantities, such as the spin susceptibility (Fig. 7) or the renormalized interaction (see SM [58]).

Interestingly, similar effects can also be observed away from half-filling, where strong magnetic fluctuations are related to a completely different type of magnetic instability. Let us repeat the calculations for the same t_{2g} model (1) for the case of $\langle N_i \rangle = 4$ and $U = 5$. Diagonal and non-diagonal components of the susceptibility are presented in Fig. 8 and SM [58], respectively. For a small value of the Hund's coupling $J = 0.2$ ($\lambda = 0.71$) the susceptibility is again nearly diagonal in the orbital space and is highly anisotropic. We also find that for the case of $\langle N_i \rangle = 4$ electrons per lattice site the spatial structure of spin fluctuations is considerably different from the half-filled case and corresponds to an incommensurate spiral state with momentum indicated in Fig. 8a by the black arrow. Nevertheless, the q_x direction still remains almost dispersionless. Increasing the value of the Hund's coupling to $J = 1$, the magnetic i.e. again approaches unity ($\lambda = 0.91$). Straightforwardly, magnetic fluctuations become isotropic and exhibit a pronounced peak at the center of the Brillouin zone (see Fig. 8b), which is associated with strong ferromagnetic (FM) fluctuations. This finding is reminiscent of the case of itinerant FM fluctuations in the d^4 compounds SrRuO₃ in its high-temperature paramagnetic phase [9, 10].

The three-point vertex corrections introduced here are the driving force for the orbitally isotropic state of the spin fluctuations. In their absence, the self-energy (5) and polarization operator (6) of the D-TRILEX approach would take the form of a simple "magnetic" GW +DMFT theory. Repeating the same calculations for the half-filled t_{2g} model without vertex corrections, we find that the i.e. of magnetic fluctuations approaches unity ($\lambda = 0.99$) already for a relatively small value of the Hund's coupling $J = 0.4$ (see SM [58]). However, the diagonal susceptibility X_{11}^{sp} remains anisotropic in momentum space. Inserting vertex corrections back, at $J = 0.4$ the leading eigenvalue reduces to $\lambda = 0.89$, but the susceptibility X_{11}^{sp} is still anisotropic and looks similar to the one calculated without vertex corrections. Finally, increasing the Hund's coupling to $J = 0.65$ results in an isotropic form of the diagonal susceptibility X_{11}^{sp} , which can be revealed in the regime of strong spin fluctuations only when vertex corrections are considered. In the case of $\langle N_i \rangle = 4$ the effect of the vertex corrections is even more substantial. At large Hund's coupling $J = 1$ the i.e. of magnetic fluctuations stays nearly the same for both considered approaches (see SM [58]). At the same time, if vertex corrections are neglected the correspond-

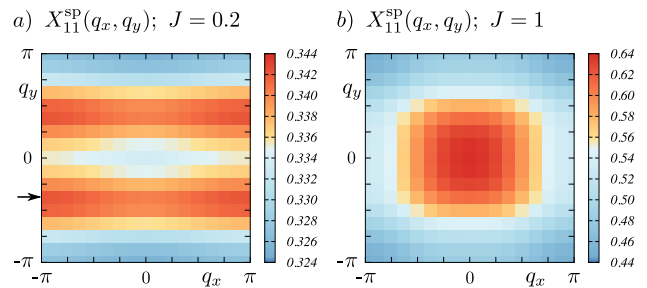


FIG. 3. The absolute value of the diagonal yz orbital component of the spin susceptibility $X_{11}^{\text{sp}}(q_x, q_y; q_z = 0, \omega = 0)$ obtained for $U = 5$ for the doped t_{2g} model. (a) For small $J = 0.2$, the diagonal susceptibility X_{11}^{sp} is highly anisotropic, and spin fluctuations correspond to an incommensurate spiral state associated with the momentum depicted by the black arrow. (b) For large $J = 1$, intraorbital spin fluctuations are isotropic and ferromagnetic as shows the symmetric bright spot at the center of the Brillouin zone.

ing magnetic mode remains incommensurate as in the regime of small Hund's coupling. On the contrary, the leading magnetic mode calculated at large $J = 1$ using the D-TRILEX approach becomes FM as discussed above. These results show that the D-TRILEX approach indeed provides a minimal consistent multi-orbital diagrammatic extension of DMFT that correctly describes collective electronic fluctuations. In contrast to other methods that rely on more complicated four-point vertex corrections which are numerically expensive and require huge memory size [60–62], in the D-TRILEX approach the four-point vertices are eliminated from the theory by using a partially bosonized approximation for the interaction [28, 33, 34]. This keeps the method computationally tractable and allows calculations even for multi-orbital systems.

Conclusions — We have studied collective spin fluctuations in a realistic strongly interacting highly anisotropic three-orbital model. We have found that the Hund's coupling enhances collective electronic effects in the spin channel. Strong magnetic fluctuations efficiently mix orbital and spatial degrees of freedom leading to orbitally isotropic behavior of the system. Remarkably, this effect emerges independently of the antiferromagnetic or ferromagnetic nature of spin fluctuations. Our findings suggest to revisit the theoretical description of collective excitations in multi-orbital materials with utmost care. On the experimental side, neutron scattering experiments should in principle be able to reveal the predicted effects. The ferromagnetic character of spin fluctuations in SrRuO₃ can be interpreted as a special case of this isotropic behavior [9, 10]. Calculations incorporating the quasi-2D nature of the electronic structure of Sr₂RuO₄ provide an interesting perspective for explaining deviations between experimental neutron scattering data and results of current theories [6, 7, 17, 18].

The authors thank Yvan Sidis, Eva Pavarini, Igor Mazin, and Josef Kaufmann for useful discussions and comments. The work of E.A.S. is supported by the Russian Science Foun-

ation Grant 18-12-00185. The work of Y.N. is supported by JSPS KAKENHI 16H06345, 17K14336, 18H01158, and 20K14423. The work of A.I.L. is supported by European Research Council via Synergy Grant 854843 - FASTCORR, by the Cluster of Excellence “Advanced Imaging of Matter” of the Deutsche Forschungsgemeinschaft (DFG) - EXC 2056 - Project No. ID390715994, and by North-German Supercomputing Alliance (HLRN) under the Project No. hhp00042. S.B. acknowledges support from the French Agence Nationale de la Recherche in the framework of the collaborative DFG-ANR project RE-MAP (Project No. 316912154) and from IDRIS/GENCI Orsay under projet t2020091393.

-
- [1] J. B. Goodenough, *Magnetism and the Chemical Bond*, Vol. 143 (Interscience (Wiley), New York, 1964).
- [2] B. Keimer, D. Casa, A. Ivanov, J. W. Lynn, M. v. Zimmermann, J. P. Hill, D. Gibbs, Y. Taguchi, and Y. Tokura, “Spin Dynamics and Orbital State in LaTiO_3 ,” *Phys. Rev. Lett.* **85**, 3946–3949 (2000).
- [3] S. N. Bushmeleva, V. Yu. Pomjakushin, D. V. Pomjakushina, E. V. and Sheptyakov, and A. M. Balagurov, “Evidence for the band ferromagnetism in SrRuO_3 from neutron diffraction,” *Journal of Magnetism and Magnetic Materials* **305**, 491–496 (2006).
- [4] K. Jenni, S. Kunkemöller, D. Brüning, T. Lorenz, Y. Sidis, A. Schneidewind, A. A. Nugroho, A. Rosch, D. I. Khomskii, and M. Braden, “Interplay of Electronic and Spin Degrees in Ferromagnetic SrRuO_3 : Anomalous Softening of the Magnon Gap and Stiffness,” *Phys. Rev. Lett.* **123**, 017202 (2019).
- [5] Y. Sidis, M. Braden, P. Bourges, B. Hennion, S. NishiZaki, Y. Maeno, and Y. Mori, “Evidence for Incommensurate Spin Fluctuations in Sr_2RuO_4 ,” *Phys. Rev. Lett.* **83**, 3320–3323 (1999).
- [6] P. Steffens, Y. Sidis, J. Kulda, Z. Q. Mao, Y. Maeno, I. I. Mazin, and M. Braden, “Spin Fluctuations in Sr_2RuO_4 from Polarized Neutron Scattering: Implications for Superconductivity,” *Phys. Rev. Lett.* **122**, 047004 (2019).
- [7] K. Jenni, S. Kunkemöller, P. Steffens, Y. Sidis, R. Bewley, Z. Q. Mao, Y. Maeno, and M. Braden, “Neutron scattering studies on spin fluctuations in Sr_2RuO_4 ,” *Phys. Rev. B* **103**, 104511 (2021).
- [8] G. Khaliullin and S. Maekawa, “Orbital Liquid in Three-Dimensional Mott Insulator: LaTiO_3 ,” *Phys. Rev. Lett.* **85**, 3950–3953 (2000).
- [9] Gertjan Koster, Lior Klein, Wolter Siemons, Guus Rijnders, J. Steven Dodge, Chang-Beom Eom, Dave H. A. Blank, and Malcolm R. Beasley, “Structure, physical properties, and applications of SrRuO_3 thin films,” *Rev. Mod. Phys.* **84**, 253–298 (2012).
- [10] A. T. Zayak, X. Huang, J. B. Neaton, and Karin M. Rabe, “Structural, electronic, and magnetic properties of SrRuO_3 under epitaxial strain,” *Phys. Rev. B* **74**, 094104 (2006).
- [11] David J. Singh, “Electronic and magnetic properties of the $4d$ itinerant ferromagnet SrRuO_3 ,” *Journal of Applied Physics* **79**, 4818–4820 (1996).
- [12] P. B. Allen, H. Berger, O. Chauvet, L. Forro, T. Jarlborg, A. Junod, B. Revaz, and G. Santi, “Transport properties, thermodynamic properties, and electronic structure of SrRuO_3 ,” *Phys. Rev. B* **53**, 4393–4398 (1996).
- [13] I. I. Mazin and D. J. Singh, “Electronic structure and magnetism in Ru-based perovskites,” *Phys. Rev. B* **56**, 2556–2571 (1997).
- [14] Jernej Mravlje, Markus Aichhorn, Takashi Miyake, Kristjan Haule, Gabriel Kotliar, and Antoine Georges, “Coherence-Incoherence Crossover and the Mass-Renormalization Puzzles in Sr_2RuO_4 ,” *Phys. Rev. Lett.* **106**, 096401 (2011).
- [15] Antoine Georges, Luca de’ Medici, and Jernej Mravlje, “Strong Correlations from Hund’s Coupling,” *Annual Review of Condensed Matter Physics* **4**, 137–178 (2013).
- [16] C. N. Veenstra, Z.-H. Zhu, M. Raichle, B. M. Ludbrook, A. Nicolaou, B. Slomski, G. Landolt, S. Kittaka, Y. Maeno, J. H. Dil, I. S. Elfimov, M. W. Haverkort, and A. Damascelli, “Spin-Orbital Entanglement and the Breakdown of Singlets and Triplets in Sr_2RuO_4 Revealed by Spin- and Angle-Resolved Photoemission Spectroscopy,” *Phys. Rev. Lett.* **112**, 127002 (2014).
- [17] Lewin Boehnke, Philipp Werner, and Frank Lechermann, “Multi-orbital nature of the spin fluctuations in Sr_2RuO_4 ,” *EPL (Europhysics Letters)* **122**, 57001 (2018).
- [18] Hugo U. R. Strand, Manuel Zingl, Nils Wentzell, Olivier Parcollet, and Antoine Georges, “Magnetic response of Sr_2RuO_4 : Quasi-local spin fluctuations due to Hund’s coupling,” *Phys. Rev. B* **100**, 125120 (2019).
- [19] Swagata Acharya, Dimitar Pashov, Cédric Weber, Hyowon Park, Lorenzo Sponza, and Mark Van Schilfgaarde, “Evening out the spin and charge parity to increase T_c in Sr_2RuO_4 ,” *Communications Physics* **2**, 163 (2019).
- [20] E. Pavarini, E. Koch, and A. I. Lichtenstein, “Mechanism for Orbital Ordering in KCuF_3 ,” *Phys. Rev. Lett.* **101**, 266405 (2008).
- [21] S. Biermann, A. Poteryaev, A. I. Lichtenstein, and A. Georges, “Dynamical Singlets and Correlation-Assisted Peierls Transition in VO_2 ,” *Phys. Rev. Lett.* **94**, 026404 (2005).
- [22] E. Pavarini, S. Biermann, A. Poteryaev, A. I. Lichtenstein, A. Georges, and O. K. Andersen, “Mott Transition and Suppression of Orbital Fluctuations in Orthorhombic $3d^1$ Perovskites,” *Phys. Rev. Lett.* **92**, 176403 (2004).
- [23] Christoph J. Halboth and Walter Metzner, “ d -Wave Superconductivity and Pomeranchuk Instability in the Two-Dimensional Hubbard Model,” *Phys. Rev. Lett.* **85**, 5162–5165 (2000).
- [24] P. Jakubczyk, W. Metzner, and H. Yamase, “Turning a First Order Quantum Phase Transition Continuous by Fluctuations: General Flow Equations and Application to d -Wave Pomeranchuk Instability,” *Phys. Rev. Lett.* **103**, 220602 (2009).
- [25] Frank Lechermann, “Multiorbital Processes Rule the $\text{Nd}_{1-x}\text{Sr}_x\text{NiO}_2$ Normal State,” *Phys. Rev. X* **10**, 041002 (2020).
- [26] Byungkyun Kang, Corey Melnick, Patrick Semon, Gabriel Kotliar, and Sangkook Choi, “Infinite-layer nickelates as Ni-eg Hund’s metals,” (2020), arXiv:2007.14610 [cond-mat.str-el].
- [27] H. Miao, Y. L. Wang, J.-X. Yin, J. Zhang, S. Zhang, M. Z. Hasan, R. Yang, X. C. Wang, C. Q. Jin, T. Qian, H. Ding, H.-N. Lee, and G. Kotliar, “Hund’s superconductor $\text{Li}(\text{Fe},\text{Co})\text{As}$,” *Phys. Rev. B* **103**, 054503 (2021).
- [28] E. A. Stepanov, V. Harkov, and A. I. Lichtenstein, “Consistent partial bosonization of the extended Hubbard model,” *Phys. Rev. B* **100**, 205115 (2019).
- [29] V. Harkov, M. Vandelli, S. Brener, A. I. Lichtenstein, and E. A. Stepanov, “Impact of partially bosonized collective fluctuations on electronic degrees of freedom,” *Phys. Rev. B* **103**, 245123 (2021).
- [30] Lars Hedin, “New Method for Calculating the One-Particle Green’s Function with Application to the Electron-Gas Problem,” *Phys. Rev.* **139**, A796–A823 (1965).

- [31] F. Aryasetiawan and O. Gunnarsson, “The *GW* method,” Reports on Progress in Physics **61**, 237 (1998).
- [32] Lars Hedin, “On correlation effects in electron spectroscopies and the *GW* approximation,” Journal of Physics: Condensed Matter **11**, R489 (1999).
- [33] E. A. Stepanov, S. Brener, F. Krien, M. Harland, A. I. Lichtenstein, and M. I. Katsnelson, “Effective Heisenberg Model and Exchange Interaction for Strongly Correlated Systems,” Phys. Rev. Lett. **121**, 037204 (2018).
- [34] E. A. Stepanov, A. Huber, A. I. Lichtenstein, and M. I. Katsnelson, “Effective Ising model for correlated systems with charge ordering,” Phys. Rev. B **99**, 115124 (2019).
- [35] M. H. Hettler, A. N. Tahvildar-Zadeh, M. Jarrell, T. Pruschke, and H. R. Krishnamurthy, “Nonlocal dynamical correlations of strongly interacting electron systems,” Phys. Rev. B **58**, R7475–R7479 (1998).
- [36] A. I. Lichtenstein and M. I. Katsnelson, “Antiferromagnetism and d-wave superconductivity in cuprates: A cluster dynamical mean-field theory,” Phys. Rev. B **62**, R9283–R9286 (2000).
- [37] Gabriel Kotliar, Sergej Y. Savrasov, Gunnar Pálsson, and Giulio Biroli, “Cellular dynamical mean field approach to strongly correlated systems,” Phys. Rev. Lett. **87**, 186401 (2001).
- [38] Thomas Maier, Mark Jarrell, Thomas Pruschke, and Matthias H. Hettler, “Quantum cluster theories,” Rev. Mod. Phys. **77**, 1027–1080 (2005).
- [39] A.-M. S. Tremblay, B. Kyung, and D. Sénéchal, “Pseudogap and high-temperature superconductivity from weak to strong coupling. Towards a quantitative theory (Review Article),” Low Temperature Physics **32**, 424–451 (2006).
- [40] G. Kotliar, S. Y. Savrasov, K. Haule, V. S. Oudovenko, O. Parcollet, and C. A. Marianetti, “Electronic structure calculations with dynamical mean-field theory,” Rev. Mod. Phys. **78**, 865–951 (2006).
- [41] E. Pavarini, A. Yamasaki, J. Nuss, and O. K. Andersen, “How chemistry controls electron localization in $3d^1$ perovskites: a Wannier-function study,” New Journal of Physics **7**, 188–188 (2005).
- [42] Yusuke Nomura, Merzuk Kaltak, Kazuma Nakamura, Ciro Taranto, Shiro Sakai, Alessandro Toschi, Ryotaro Arita, Karsten Held, Georg Kresse, and Masatoshi Imada, “Effective on-site interaction for dynamical mean-field theory,” Phys. Rev. B **86**, 085117 (2012).
- [43] Junjiro Kanamori, “Electron Correlation and Ferromagnetism of Transition Metals,” Progress of Theoretical Physics **30**, 275–289 (1963).
- [44] Thomas Ayrál, Jaska Vučičević, and Olivier Parcollet, “Fierz convergence criterion: A controlled approach to strongly interacting systems with small embedded clusters,” Phys. Rev. Lett. **119**, 166401 (2017).
- [45] Antoine Georges, Gabriel Kotliar, Werner Krauth, and Marcelo J. Rozenberg, “Dynamical mean-field theory of strongly correlated fermion systems and the limit of infinite dimensions,” Rev. Mod. Phys. **68**, 13–125 (1996).
- [46] A. N. Rubtsov, M. I. Katsnelson, and A. I. Lichtenstein, “Dual boson approach to collective excitations in correlated fermionic systems,” Annals of Physics **327**, 1320 – 1335 (2012).
- [47] Erik G. C. P. van Loon, Alexander I. Lichtenstein, Mikhail I. Katsnelson, Olivier Parcollet, and Hartmut Hafermann, “Beyond extended dynamical mean-field theory: Dual boson approach to the two-dimensional extended Hubbard model,” Phys. Rev. B **90**, 235135 (2014).
- [48] E. A. Stepanov, E. G. C. P. van Loon, A. A. Katanin, A. I. Lichtenstein, M. I. Katsnelson, and A. N. Rubtsov, “Self-consistent dual boson approach to single-particle and collective excitations in correlated systems,” Phys. Rev. B **93**, 045107 (2016).
- [49] E. A. Stepanov, A. Huber, E. G. C. P. van Loon, A. I. Lichtenstein, and M. I. Katsnelson, “From local to nonlocal correlations: The Dual Boson perspective,” Phys. Rev. B **94**, 205110 (2016).
- [50] L. Peters, E. G. C. P. van Loon, A. N. Rubtsov, A. I. Lichtenstein, M. I. Katsnelson, and E. A. Stepanov, “Dual boson approach with instantaneous interaction,” Phys. Rev. B **100**, 165128 (2019).
- [51] M. Vandelli, V. Harkov, E. A. Stepanov, J. Gukelberger, E. Kozik, A. Rubio, and A. I. Lichtenstein, “Dual boson diagrammatic Monte Carlo approach applied to the extended Hubbard model,” Phys. Rev. B **102**, 195109 (2020).
- [52] C.-O. Almbladh, U. von Barth, and R. van Leeuwen, “Variational total energies from Φ - and Ψ - Derivable Theories,” International Journal of Modern Physics B **13**, 535–541 (1999).
- [53] In order to make the first implementation of the multi-orbital D-TRILEX theory simple, we do not consider the renormalization of the non-local self-energy by a “dual” denominator [28], because it does not qualitatively affect described effects.
- [54] For this reason, in Ref. 28 the method was called TRILEX² approximation for the DB theory.
- [55] Thomas Ayrál and Olivier Parcollet, “Mott physics and spin fluctuations: A unified framework,” Phys. Rev. B **92**, 115109 (2015).
- [56] Thomas Ayrál and Olivier Parcollet, “Mott physics and spin fluctuations: A functional viewpoint,” Phys. Rev. B **93**, 235124 (2016).
- [57] J. Kaufmann et al., to be published.
- [58] See Supplemental Material at <http://> for the non-local Green’s function, the non-diagonal part of the susceptibility, the renormalized spin interaction, and the illustration of the importance of vertex corrections.
- [59] In order to get such large leading eigenvalue we reduce the threshold for the self-consistency to 10 iterations. Otherwise, it would require a more precise adjustment of the temperature and the Hund’s coupling.
- [60] Anna Galler, Patrik Thunström, Patrik Gunacker, Jan M. Tomczak, and Karsten Held, “*Ab initio* dynamical vertex approximation,” Phys. Rev. B **95**, 115107 (2017).
- [61] Anna Galler, Josef Kaufmann, Patrik Gunacker, Matthias Pickem, Patrik Thunström, Jan M. Tomczak, and Karsten Held, “Towards *ab initio* Calculations with the Dynamical Vertex Approximation,” Journal of the Physical Society of Japan **87**, 041004 (2018).
- [62] Josef Kaufmann, Christian Eckhardt, Matthias Pickem, Motoharu Kitatani, Anna Kauch, and Karsten Held, “Self-consistent ladder dynamical vertex approximation,” Phys. Rev. B **103**, 035120 (2021).

Supplemental Material

Orbital Isotropy of Magnetic Fluctuations in Correlated Electron Materials Induced by Hund's Exchange Coupling

Nondiagonal component of the spin susceptibility

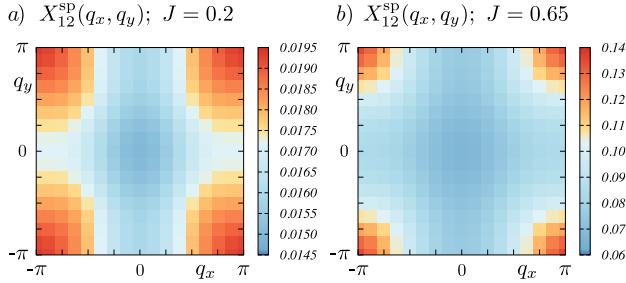


FIG. 4. The absolute value of the nondiagonal component of the spin susceptibility X_{12}^{SP} on the $(q_x, q_y; q_z = 0, \omega = 0)$ plane obtained for the half-filled t_{2g} model.

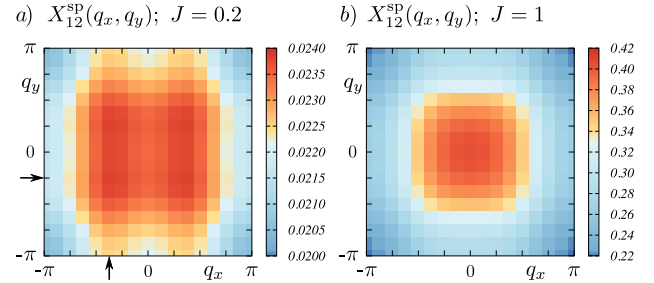


FIG. 5. The absolute value of the nondiagonal component of the spin susceptibility X_{12}^{SP} on the $(q_x, q_y; q_z = 0, \omega = 0)$ plane obtained for the case of 4 electrons per lattice site.

In this section we show the nondiagonal part of the spin susceptibility $X_{12}^{\text{SP}}(q_x, q_y; q_z = 0; \omega = 0)$, where indices 1 and 2 correspond to yz and zx orbitals, respectively. In the half-filled case $\langle N_i \rangle = 3$ and small Hund's coupling $J = 0.2$ (Fig. 4 a) this quantity is almost isotropic, but negligibly small compared to the diagonal component of the susceptibility X_{11}^{SP} shown in the main text. On the contrary, for large Hund's coupling $J = 0.65$ and the same filling $\langle N_i \rangle = 3$ the nondiagonal part of the spin susceptibility is fully isotropic with the pronounced antiferromagnetic behavior (see Fig. 4 b), and its amplitude is comparable to the one of the X_{11}^{SP} . A similar behavior of the nondiagonal spin susceptibility can also be found for the filling of $\langle N_i \rangle = 4$ electrons per lattice site shown in Fig. 5. In this case, for small $J = 0.2$ interorbital spin fluctuations correspond to an incommensurate spiral state associated with momenta depicted by black arrows. For large $J = 1$, interorbital spin fluctuations are isotropic and ferromagnetic as shows the symmetric bright spot at the center of the Brillouin zone.

Nonlocal Green's function at half-filling

In this section we show the imaginary part of the nonlocal Green's function obtained for the half-filled case. Fig. 6 illustrates that for both values of the Hund's coupling (a) $J = 0.2$ and (b) $J = 0.65$ the Green's function remains anisotropic in momentum space, as follows from the discussion presented in the main text of the paper.

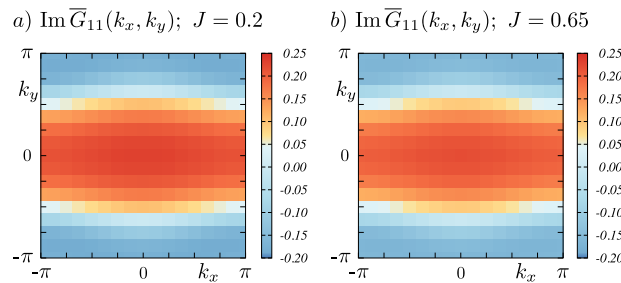


FIG. 6. Imaginary part of the nonlocal Green's function $\overline{G}_{11}(k_x, k_y; k_z = 0, \nu = \pi/\beta)$ for the yz orbital obtained for the half-filled t_{2g} model.

Renormalized spin interaction

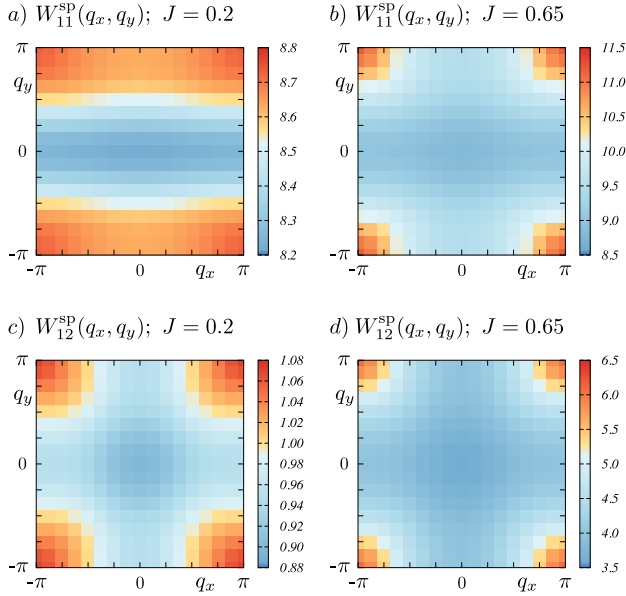


FIG. 7. The absolute value of the diagonal (a, b) and non-diagonal (c, d) components of the renormalized spin interaction $W_{ll'}^{SP}(q_x, q_y; q_z = 0, \omega = 0)$ obtained for the half-filled case.

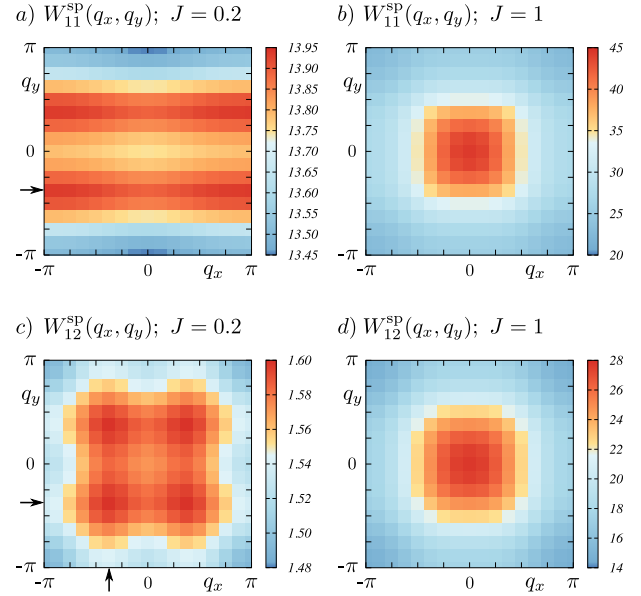


FIG. 8. The absolute value of the diagonal (a, b) and non-diagonal (c, d) components of the renormalized spin interaction $W_{ll'}^{SP}(q_x, q_y; q_z = 0, \omega = 0)$ obtained for the filling $\langle N_i \rangle = 4$.

The anisotropic to isotropic transition of magnetic fluctuations, which has been captured by the spin susceptibility $X_{ll'}^{SP}$, can also be seen in the renormalized spin interaction $W_{ll'}^{SP}$ that directly enters the electronic self-energy (see Eq. 5 of the main text). Both, $X_{ll'}^{SP}$ and $W_{ll'}^{SP}$ quantities are obtained via similar Dyson equations

$$X_{ll'}^{SP-1}(q) = \Pi_{ll'}^{SP-1}(q) - U_{ll'}^{SP} \quad (7)$$

$$W_{ll'}^{SP-1}(q) = U_{ll'}^{SP-1} - \Pi_{ll'}^{SP}(q) \quad (8)$$

For this reason, the structure of the renormalized spin interaction shown in Fig. 7 for the half-filled case and in Fig. 8 for the case of $\langle N_i \rangle = 4$ electrons per lattice site is very similar to the one of the spin susceptibility. Moreover, one may notice that the nondiagonal part of the renormalized spin interaction W_{12}^{SP} for both values of the Hund's coupling, as well as the diagonal interaction W_{11}^{SP} at large J look more isotropic compared to the corresponding components of the spin susceptibility. This observation can be explained by the fact that the local bare interaction $U_{ll'}^{SP}$ gives the first-order contribution to the renormalized interaction $W_{ll'}^{SP}(q)$. On the contrary, the first-order contribution to the spin susceptibility $X_{ll'}^{SP}(q)$ is given by the polarization operator $\Pi_{ll'}^{SP}(q)$, which in this particular model is anisotropic as discussed in the main text of the paper.

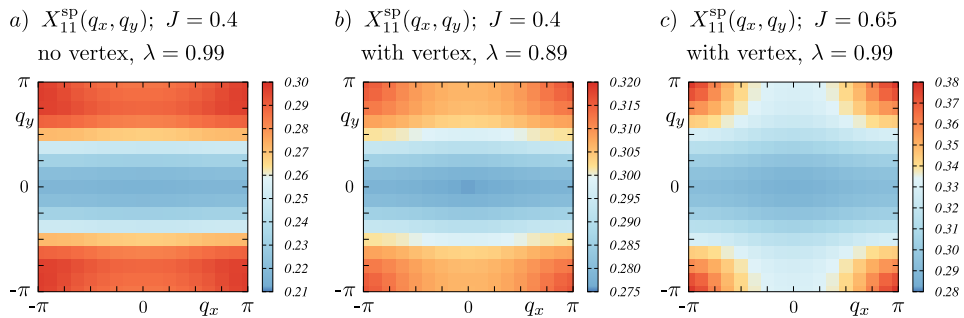


FIG. 9. The absolute value of the diagonal component of the spin susceptibility $X_{11}^{SP}(q_x, q_y; q_z = 0, \omega = 0)$ calculated for the half-filled case.

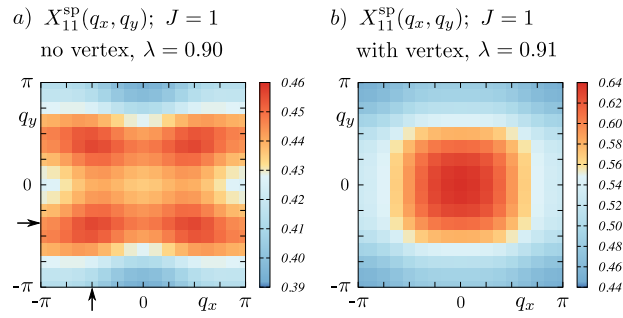


FIG. 10. The absolute value of the diagonal component of the spin susceptibility $X_{11}^{\text{sp}}(q_x, q_y; q_z = 0, \omega = 0)$ calculated for the case of $\langle N_i \rangle = 4$ electrons per lattice site and $J = 1$.

Effect of vertex corrections

In this section we illustrate the importance of vertex corrections considered in the D-TRILEX diagrams for the self-energy (Eq. 5 in the main text) and polarization operator (Eq. 6 in the main text). To this aim we first obtain the spin susceptibility for the half-filled case without (Fig. 9 a) and with (Fig. 9 b, c) vertex corrections. Without vertices, the leading eigenvalue of magnetic fluctuations approaches unity ($\lambda = 0.99$) already for a relatively small value of the Hund's coupling $J = 0.4$. As Fig. 9 a shows, in this case the diagonal part of the spin susceptibility X_{11}^{sp} still remains anisotropic in the $(q_x, q_y; q_z = 0)$ plane. Including vertex corrections, the leading eigenvalue reduces to $\lambda = 0.89$ for the same value of the Hund's coupling $J = 0.4$. The corresponding spin susceptibility X_{11}^{sp} shown in Fig. 9 b also remains anisotropic and looks similar to the one calculated without vertex corrections. Increasing the Hund's coupling to $J = 0.65$ allows one to obtain the isotropic form of the spin susceptibility X_{11}^{sp} , which can be revealed in the regime of strong spin fluctuations ($\lambda = 0.99$) *only* if vertex corrections are considered.

In the case of $\langle N_i \rangle = 4$ electrons per lattice site the effect of the vertex corrections is even more demonstrative. Calculating the spin susceptibility for large Hund's coupling $J = 1$ without (Fig. 10 a) and with (Fig. 10 b) vertex corrections in diagrams for the self-energy and polarization operator one finds approximately the same leading eigenvalue of magnetic fluctuations. At the same time, without vertices spin fluctuations correspond to an incommensurate spiral state associated with the momentum depicted by the black arrows in Fig. 10 a. Inclusion of vertex corrections drastically changes the symmetry of the spin fluctuations, and the leading magnetic mode becomes ferromagnetic (Fig. 10 b).